

Puerto Lápice eucrite fall: Strewn field, physical description, probable fireball trajectory, and orbit

Josep M. TRIGO-RODRÍGUEZ^{1,2*}, Jiří BOROVIČKA³, Jordi LLORCA⁴, José M. MADIEDO^{5,6},
Jaime ZAMORANO⁷, and Jaime IZQUIERDO⁷

¹Institut de Ciències de l'Espai-CSIC. Campus UAB, Facultat de Ciències, Torre C5-p2, 08193, Spain

²Institut d'Estudis Espacials de Catalunya (IEEC), Gran Capità 2–4, Ed. Nexus. 08034 Barcelona, Spain

³Astronomical Institute, Academy of Sciences, Ondřejov Observatory, Czech Republic

⁴Institut de Tècniques Energètiques, Universitat Politècnica de Catalunya (UPC), Spain;

⁵Facultad de Ciencias Experimentales, Universidad de Huelva, Huelva, Spain

⁶CIECEM, Universidad de Huelva, Parque Dunar s/n, 21760 Almonte, Spain

⁷Departamento de Astrofísica y CC. de la Atmósfera, Facultad Ciencias Físicas, Universidad Complutense de Madrid, Spain

*Corresponding author. E-mail: trigo@aliga.ieec.uab.es

(Received 10 July 2008; revision accepted 14 December 2008)

Abstract—The fall of the Puerto Lápice eucrite occurred on May 10, 2007, at 17 h 57 m 30 ± 30 s UTC. Its daylight fireball was witnessed by hundreds of people from Spain, and produced a meteorite fall associated with a large strewn field of fragments. There were no direct pictures of the fireball, but several pictures of the fireball's train were taken from different locations in Spain. Additional theodolite calibrations of visual records were made in order to find the most probable fireball trajectory based on the available data. The shape of the meteorite strewn field was considered as well. Although the orbit of the Puerto Lápice meteoroid could not be computed due to the absence of velocity data, we assumed a likely range of geocentric velocities and computed a range of possible orbits. All solutions show that the body was in an Apollo-type orbit, with low inclination and perihelion distance just below 1 astronomical unit (AU). This is the first case that an orbit can be discussed for an HED meteorite fall.

INTRODUCTION

The fall of the Puerto Lápice meteorite (Connolly et al. 2008; Madiedo et al. 2008) occurred near a small town with the same name located in the north of the province of Ciudad Real, Spain, on Thursday, May 10, 2007, at 17 h 57 m 30 s ± 30 s UTC. The original meteoroid suffered multiple fragmentations during its entry, and the survival of some pieces produced a meteorite fall associated with a large strewn field of fragments. The fireball appeared in broad daylight when hundreds of people had just left work to go home. The event was studied by the Spanish Meteor and Fireball Network (SPMN) which previously recovered the Villalbeto de la Peña chondrite (Llorca et al. 2005; Trigo-Rodríguez et al. 2006). Although this bolide overflew some of the less populated provinces of Spain, because it was so bright, the event was also seen from some of the most populated cities, e.g., Barcelona, Madrid, Valencia, etc. The SPMN received more than two hundred eyewitness reports of the fireball that arrived from sites located even at distances larger than 900 km, e.g., two locations placed in the

Barcelona and Sevilla provinces. Two days after the fall, SPMN researchers interviewed eyewitnesses in Ciudad Real province in order to get a preliminary trajectory of the fireball. Our first estimates of the luminous trajectory ending below a height of 25 km were indicative of a probable meteorite fall.

Llorca et al. (2008) characterized this meteorite as an eucrite. Since no detailed trajectory and orbital information has so far been reported of a HED meteorite, we have put all our effort in reconstructing the atmospheric trajectory of this meteorite. The importance lies in the fact that only 33 eucrites had been observed to fall until July 2008 (The Meteoritical Bulletin Database) and no valuable trajectory and orbital data were obtained in previous cases, except for some marginal trajectory information compiled by Nininger (1936) on the Pasamonte eucrite fall on March 24, 1933. Consequently, the Puerto Lápice meteorite fall is a unique opportunity for obtaining new clues on the origin of eucrites. Photographs of the fireball train and visual reports collected by the SPMN, together with the accurate determination of the location of 67 recovered meteorites, provide some clues to the origin of Puerto Lápice eucrite. In this paper, based on all available

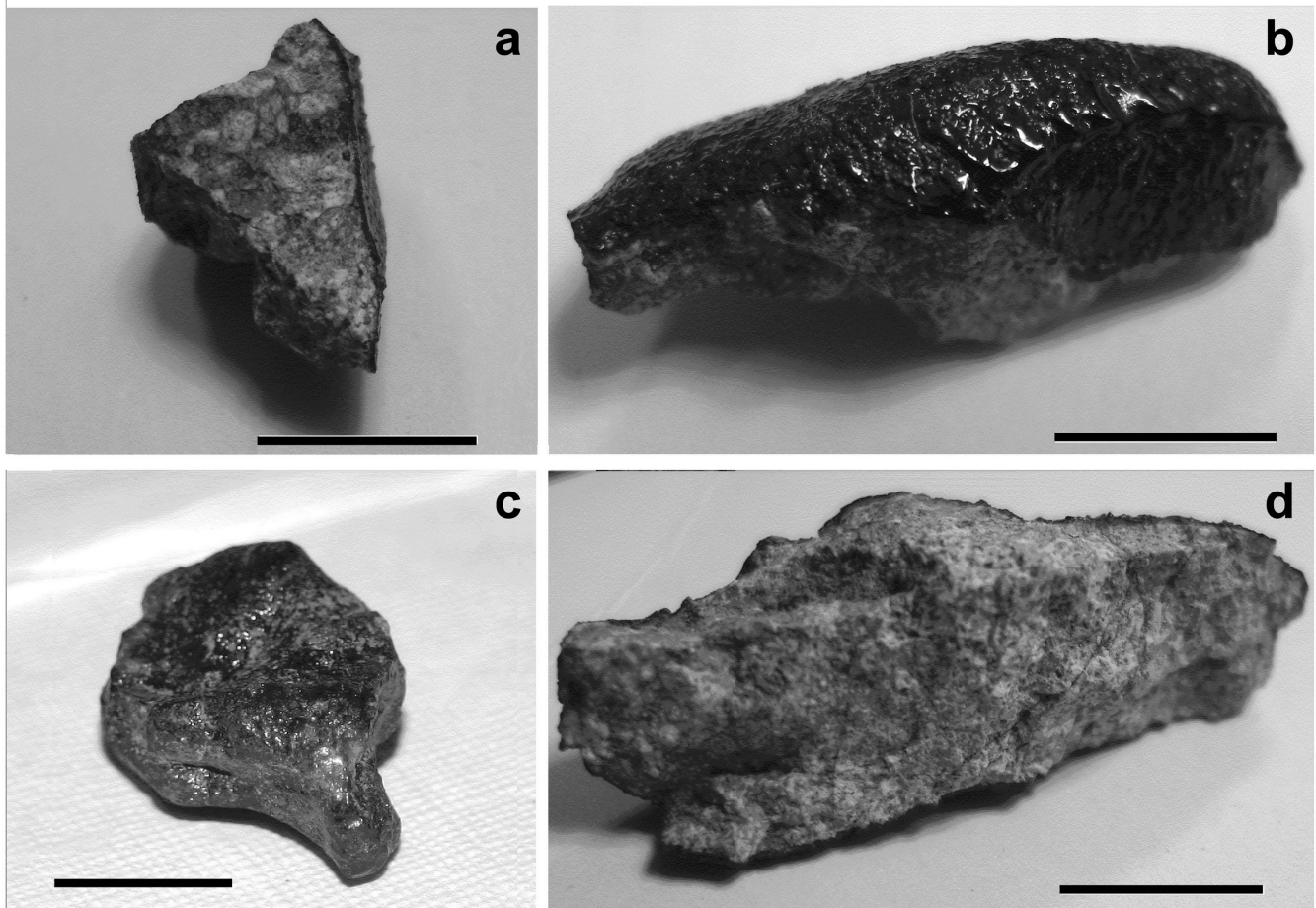


Fig. 1. Different specimens recovered of the Puerto Lápice eucrite. A centimeter-size black scale is included in each picture. a) Fragmented piece showing a brecciated structure, and the presence of different clast types, each with distinct textural features. A very thin fusion crust covers the right side of this piece. b) Another piece showing an orientated flight pattern in the fusion crust. c) Irregular piece exhibiting a complete fusion crust. d) Bottom of the piece shown in (b) where it is evident that a crack crosses the sample.

data, we focus on the determination of the fireball's atmospheric trajectory and the heliocentric orbit of the progenitor meteoroid.

METEORITE DESCRIPTION AND RECONSTRUCTED STREWN FIELD

Most of the recovered specimens were identified because part of their surface is covered by a shiny fusion crust. The interior is white but brecciated, showing dark and clear areas that can be typically distinguished by eye (Fig. 1a). Table 1 compile the positions, and masses of all recovered meteorites to our knowledge that represent a total known weight of 468.8 grams. About 60% of the pieces were broken, and almost all of them exhibited irregular shapes (Figs. 1b–c). Eyewitnesses' descriptions of the Puerto Lápice fireball and the available pictures of the persistent train left by the fireball in the atmosphere suggest that the meteoroid experienced successive fragmentations during its descent through the atmosphere. These resulted in a complex and heterogeneous

distribution of the pieces on the ground. Although some pieces broke when they impacted the ground, it seems likely that most of them broke apart during the last stages of flight. Evidence for this is the fact that different pieces that were separated by a few meters were located on the ground aligned in the direction of the preferential wind pattern. Some examples are meteorites #29, 30, 31, and 32 (Table 1); #29 (5 g) is in the front of the distribution, and #32 (0.8 g) is in the tail. Every time that a large piece was found, we traced spirals around it searching for smaller ones. Typically, the pieces appeared aligned in the direction of the wind.

Meteorite recovery tasks were complicated due to the hot weather, and the intrinsic difficulties associated with the landing area, covered by large stones and being mostly vineyards and olive tree fields. In addition, about 90% of the strewn field was ploughed in the following three months so the strewn field shown in Fig. 2 is clearly biased by these factors. Despite these problems, Puerto Lápice is one of the best sampled strewn fields obtained for a eucrite. This case exemplifies how the catastrophic disruption of the main body along the atmospheric trajectory can produce an

Table 1. Geographic coordinates, and masses of the known recovered meteorites. The total known weight was 468.8 g. The largest recovered piece was fragment#18.

Meteorite #	Long.W (°)	Lat. N (°)	Altitude (m)	Mass (g)
1	3.5220	39.3648	730	5.7
2	3.5219	39.3625	730	4.5
3	3.5226	39.3618	735	3
4	3.5212	39.3619	730	3.8
5	3.5227	39.3614	730	5.9
6	3.5229	39.3633	728	2.0
7	3.5153	39.3585	727	2.5
8	3.5153	39.3585	727	5.6
9	3.517	39.3701	726	1.1
10	3.5181	39.3565	730	0.1
11	3.5250	39.3632	730	8.4
12	3.5181	39.3565	726	4.3
13	3.5316	39.3660	765	4.6
14	3.5387	39.3642	775	6.3
15	3.5384	39.3645	770	2.5
16	3.5413	39.3643	765	29.4
17	3.5443	39.3647	770	12.1
18	3.5477	39.3672	775	89.1
19	3.5492	39.3662	775	12.1
20	3.5460	39.3673	770	22.6
21	3.5149	39.3531	725	3.2
22	3.5182	39.3532	725	11.1
23	3.5166	39.3531	730	5.8
24	3.5163	39.3532	730	8.3
25	3.5189	39.3534	730	6.9
26	3.5170	39.3547	725	4.5
27	3.5164	39.3562	735	1.9
28	3.5099	39.3513	713	2.5
29	3.5158	39.3573	722	5.0
30	3.5157	39.3575	722	3.5
31	3.5156	39.3573	722	2.4
32	3.5156	39.3572	720	0.8
33	3.5169	39.3571	720	2.9
34	3.5169	39.3577	720	4.4
35	3.5138	39.3578	720	5.6
36	3.5158	39.3562	725	1.3
37	3.5173	39.3566	725	2.5
38	3.5183	39.3535	720	3.0
39	3.5187	39.3542	720	4.1
40	3.5201	39.3542	720	2.9
41	3.5178	39.3543	720	5.6
42	3.5321	39.3688	720	5.2
43	3.5141	39.3587	720	1.9
44	3.5109	39.3534	720	3.2
45	3.5198	39.3487	720	5.1
46	3.5164	39.3562	738	1.3
47	3.5172	39.3561	738	8.0
48	3.5178	39.3509	723	13.7
49	3.5198	39.3487	725	5.2
50	3.5287	39.3478	739	5.2
51	3.5288	39.3481	739	3.4
52	3.5246	39.3523	722	6.7
53	3.5236	39.3519	722	10.4

Table 1. *Continued.* Geographic coordinates, and masses of the known recovered meteorites. The total known weight was 468.8 g. The largest recovered piece was fragment#18.

Meteorite #	Long.W (°)	Lat. N (°)	Altitude (m)	Mass (g)
54	3.5242	39.3497	721	6.1
55	3.5259	39.3505	735	7.0
56	3.5252	39.3503	730	10.2
57	3.5238	39.3501	725	5.6
58	3.5236	39.3486	725	4.8
59	3.5213	39.3477	725	1.4
60	3.5213	39.3476	725	6.0
61	3.5206	39.3477	725	6.1
62	3.5181	39.3498	725	3.0
63	3.5215	39.3518	723	10.5
64	3.5172	39.3487	725	9.7
65	3.5164	39.3484	725	6.7
66	3.5122	39.3494	720	4.7
67	3.5118	39.3497	720	3.9

extremely large (and difficult) recovery area. As a consequence of the complexity involved in the fragmentation of the pieces, the meteorite distribution was highly heterogeneous for those areas inspected before they were ploughed. The largest piece recovered in the front of the strewn field has a mass of 89.1 grams, while two other pieces behind it have masses over 20 grams, and another three are over 10 grams. These meteorites are exceptional because about 85% of the recovered pieces have masses below 6 grams (see Table 1). The catastrophic fragmentation of the original rock produced pieces sufficiently large to survive, but others were likely too small to prevent their complete ablation. The smallest pieces recovered have masses of only 1 and 0.1 g (Table 1). Our data are particularly relevant because there is little information about strewn fields of eucrites in the literature. Probably one of the most famous eucrite falls until now was Pasamonte, but only a few specimens were recovered and the strewn field was never studied in detail (Nininger 1936). Another case (from a find) that would exemplify a similarly complex and heterogeneous meteorite distribution is the Camel Donga eucrite shower from which about 600 mainly crusted individuals were recovered (Grossman and Score 1996).

PHYSICAL PROPERTIES OF THE METEORITES

Physical examination of the meteorite specimens showed that most fragments have a thick, glassy, and shiny fusion crust typical of calcium-rich eucrites. The fusion crust ranges from 0.8 to about 3 mm in thickness. Figure 1 shows some of the recovered fragments. On some surfaces the fusion crust exhibits flow lines that terminate in a lip that curves around to the rear side of the fragment (Fig. 1b). In some specimens several generations of the crust indicate multiple fragmentation events. The brecciated structure of cut surfaces of various specimens was described in detail by Llorca et al. (2008).

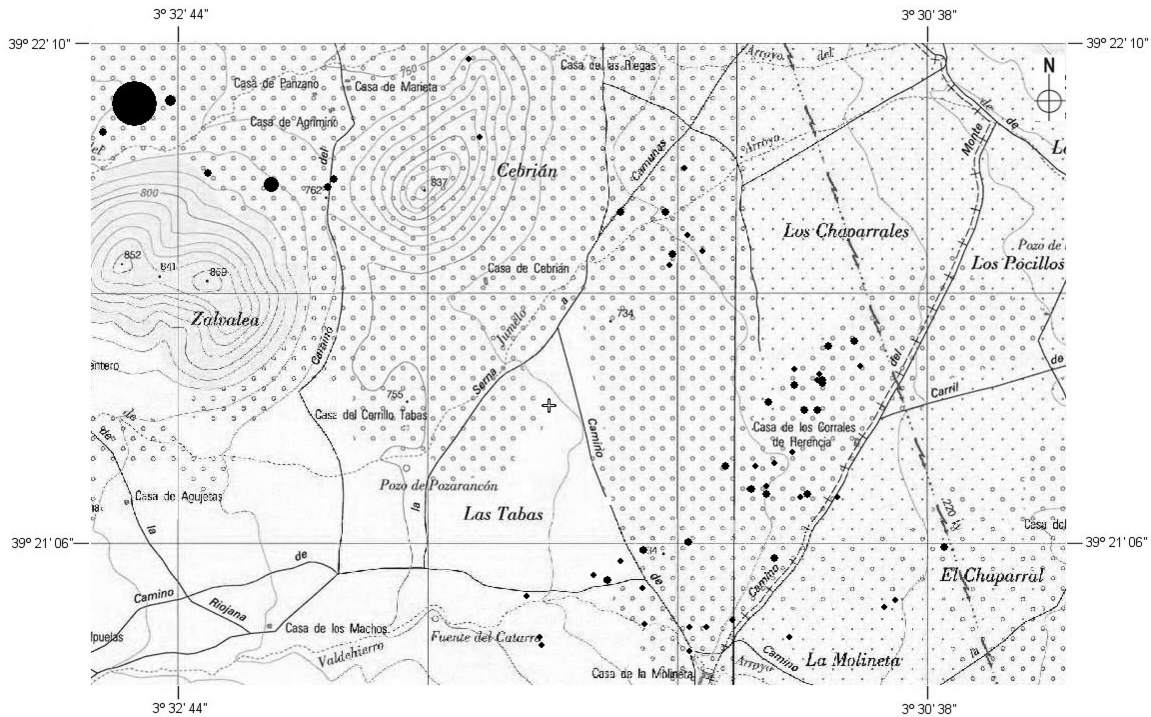


Fig. 2. Meteorite strewn field and geographic setting of the landing area. Black dots are the meteorite locations that have diameter approximately proportional to their sizes. Among the vegetation features: open circles represent olive trees and small dots indicate vineyards. The common names of the rural properties are also given for reference.

Three meteorite specimens were used for density determination. The bulk density of the Puerto Lápice meteorite is $3.12 \pm 0.10 \text{ g cm}^{-3}$, and the grain density determined with a helium pycnometer (ρ_g , density that excludes pores and voids) is $3.28 \pm 0.05 \text{ g cm}^{-3}$. From these values, the porosity of Puerto Lápice was calculated to be 4.9%. Typical grain densities reported for eucrites are within the range $3.20\text{--}3.33 \text{ g cm}^{-3}$ (Consolmagno et al. 2006). Magnetic susceptibility and grain density are commonly correlated for meteorite falls since both are intensive variables that vary with iron content (Britt et al. 2003; Consolmagno et al. 2006). The specific magnetic susceptibility, χ , of the Puerto Lápice meteorite is $\log \chi = 2.6 \pm 0.1$ (in $10^{-9} \text{ m}^3 \text{ kg}^{-1}$) (Llorca et al. 2008). The values of magnetic susceptibility and grain density of the Puerto Lápice meteorite plot well within the eucrite group in a $\log \chi$ versus ρ_g graph for meteorite falls (Consolmagno et al. 2006).

AVAILABLE TRAJECTORY DATA

Unfortunately, no direct pictures or videos of the fireball itself are known despite all SPMN search efforts of public or private security recorders. Fortunately, casual pictures of the train that remained visible for about 15 minutes after the fireball's disappearance were taken. The most valuable picture of the dusty train left in the atmosphere by the fireball was taken in the Parla district of Madrid shortly after the

disappearance of the fireball. It is shown in Fig. 3. The train is relatively straight and shows a number of brightness enhancements. Those features were numbered 1–9 and called knots. Knots 2, 6, and 7 are the brightest. Knot 7 lies a little off the line. This may be due to fireball splitting by fragmentation or due to differential drift of the train. The first option is more probable because the picture was taken only few seconds after the fireball appearance. In addition to knots 1–9, a possible knot 0 lying far in front of the other knots was measured. The signal is very faint and it is not clear if knot 0 is real part of the train or a random background noise enhancement. The coordinates of the knots (azimuth and elevation) were obtained by taking a night-time picture containing stars from the same site and measuring the coordinates of terrestrial reference objects seen on the original train picture.

Two pictures of the train were taken in Ciudad Real six minutes after the fireball and 14 seconds apart each other. The first of these images is shown in Fig. 4. Six minutes after the fireball, the train was already distorted and the direction of fireball flight cannot be inferred directly from these images. The train consists of individual diffuse clouds, which have been marked A to J. Cloud B was out of the field of view and clouds A, I, and J are hardly visible in the second image. Also, in this case, the cloud coordinates were obtained by taking a nighttime picture of the same field.

Although the smoky train apparently disappeared by contrast in the daylight illuminated atmosphere, more than

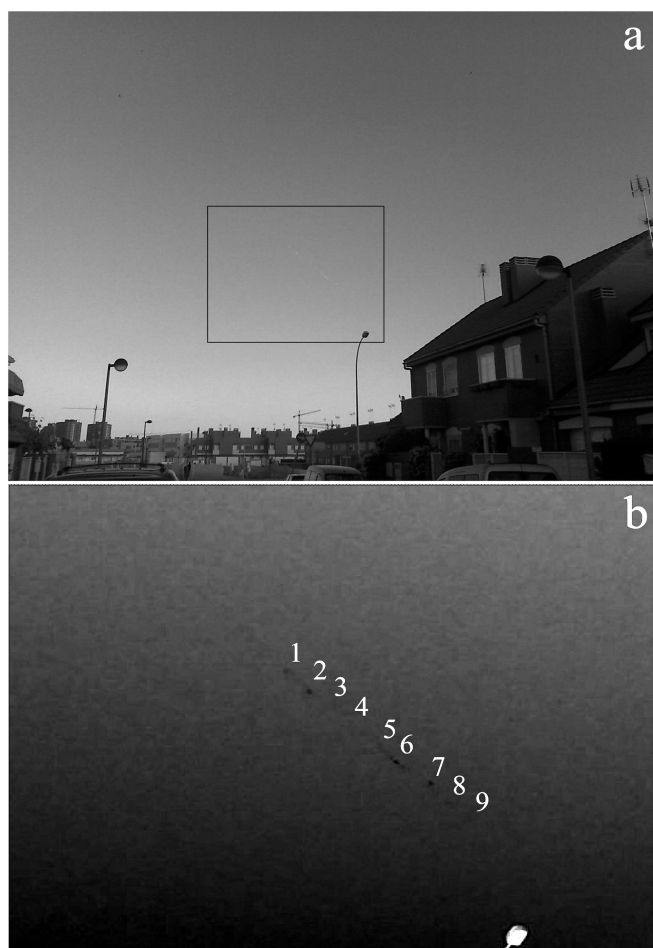


Fig. 3. The image of the fireball's train taken from Parla (Madrid) with the camera of a cell phone, converted to black-and-white. a) The original frame where several buildings and horizon details are clearly visible. Since the train was quite faint due to the relative distance and the brightness of the daylight sky, the section containing the train was enhanced in contrast and inverted. b) The magnification of the train section with the train knots numbered. Image courtesy of Manuel Trigo.

one hour after the fall, a complex dusty train appeared again, illuminated by the rays of the Sun after sunset. One picture taken from Murcia at about 19 h 15 m UT is shown in Fig. 5. At that time, the train structure was very complicated and could not be used for fireball trajectory determination.

From about 100 reports of fireball eyewitnesses obtained by e-mail, we picked up twelve reports with good references of the fireball in relation to obstacles or horizon details. The eyewitnesses were interviewed on site and the indicated positions of the fireball's beginning and end were measured using a theodolite. The summary of the visited sites is given in Table 2.

The preliminary trajectory was obtained a couple of weeks after the fall. A meteorite hunter (T. Grau) found the first meteorite in early June, being presented to the international meteor community during the Meteoroids 2007

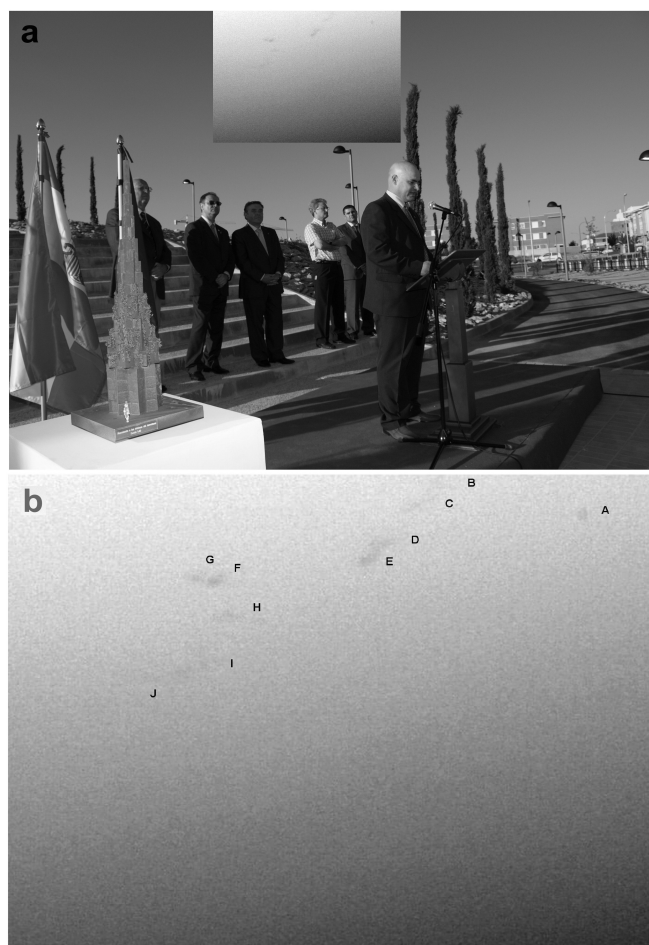


Fig. 4. Ciudad Real train images converted to black-and-white. a) First picture taken at 18 h 02 m 6 ± 1 s UTC where the part showing the fireball's train was inverted and the contrast was enhanced. b) Magnification of the enhanced window shown in (a) containing the train section with the train knots numbered. Image courtesy of Miguel A. Bajo Cabezas.

conference (Trigo-Rodríguez et al. 2008). A couple of weeks later, the area suffered flooding due to intense rain. For this reason, extensive meteorite recovery activities were delayed until the end of June. The searches were complicated due to the characteristics of the landing area, mostly plough land covered by vineyards, and olive tree fields. In addition, about 90% of the strewn field was ploughed in the following three months. Since then, several SPMN expeditions to the meteorite strewn field have allowed the recovery of 20 specimens exhibiting a shiny fusion crust, and a nice interior showing different lithologies (Llorca et al. 2008). Numerous meteorite hunters traveled to the strewn field area and removed at least 50 more pieces, and most of them were contacted for data completion and provided part of the data shown in Table 1. By using the available meteorite locations we have obtained Fig. 2. The orientation of the meteorite strewn field was used to constrain the fireball trajectory.



Fig. 5. Image of the train taken after the sunset from Murcia, converted to black-and-white and contrast enhanced. Image courtesy of Ramón Zaragoza. Color version of the image is available in the online edition.

Table 2. Details of the photographic records, and casual eyewitnesses interviewed for determining the trajectory of the Puerto Lápice fireball.

Site	Longitude W (°)	Latitude N (°)	Altitude (m)	Field of view (°)	Trajectory record length	No. of positions (head/train)	Image format
Alcantarilla, Murcia	1.11089	37.85105	216	–	All	2	Visual
Argamasilla, Ciudad Real	4.08222	38.73303	672	–	All	2	Visual
Azuqueca, Guadalajara	3.26583	40.56361	625	–	All	2	Visual
Ciudad Real	3.92428	38.99742	627	61 × 46	Ending	11	Digital
Ciudad Real	3.91472	38.99694	630	–	All	2	Visual
Dúdar, Granada	2.48092	37.17997	998	–	All	2	Visual
Madrid-c/Manipa	3.64486	40.44117	705	–	All	2	Visual
Madrid-c/ Arturo Soria	3.66778	40.47083	707	–	All	4	Visual
Majadahonda, Madrid	3.86733	40.44881	670	–	All	2	Visual
Miguelturra, Ciudad Real	3.88989	38.96292	644	–	All	2	Visual
Parla, Madrid	3.75381	40.22759	644	36 × 27	Complete smoky train	10	Digital
Pinto, Madrid	3.69881	40.25581	587	–	All	2	Visual
Puertollano, Ciudad Real	4.07677	38.68015	662	–	All	2	Visual
Soneja, Castellón	0.41917	39.81722	240	–	All	2	Visual

The high-altitude wind profile for the time and location of the fireball was modeled by the Instituto Nacional de Meteorología (INM) on the basis of a standard procedure. This model was also tested by being compared with the wind measurements obtained from an atmospheric sounding experiment performed in Madrid. From both data we obtained the wind profile given in Fig. 6. The prevailing wind direction was from west-northwest with the speed exceeding 20 m/s at a height of around 30 km. The wind profile was used to

estimate the wind-distortion of the train and the wind-driven drift of the meteorites during the dark flight.

The different clouds visible in the pictures of the persistent train demonstrate that the fireball suffered several fragmentations along its atmospheric luminous trajectory. Indeed, several sonic booms were audible from different locations in the Spanish provinces of Ciudad Real and Toledo. The early stages of fireball flight in the atmosphere also produced electrophonic sound. We have searched for fireball

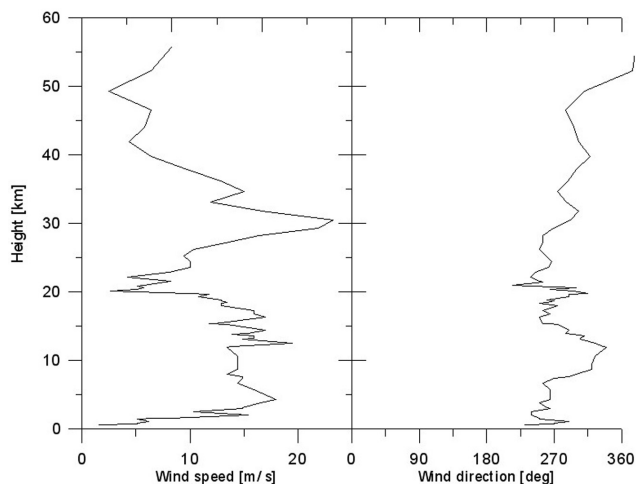


Fig. 6. High wind profile for the date and location of the fireball. Source INM.

signatures in the records of Spanish seismic stations. Unfortunately, all stations were located quite far from the fireball trajectory (more than 100 km) and no signals that could be associated with the fireball were found.

TRAJECTORY DETERMINATION

The instrumental data are not sufficient to determine the fireball trajectory by standard methods. The Parla image was central to this analysis and used to define a plane containing the fireball trajectory. The position of the middle of the meteorite strewn field was used to determine one point on the fireball trajectory. The drift caused by winds during the meteorite dark flight was taken into account. The drift was estimated to be 0.070 degrees to the east and 0.005 degrees to the south. The position of the center of the strewn field was therefore shifted in the opposite direction. A vertical line was drawn from that point. The intersection of that line with the Parla plane defines what we call the meteor point. The coordinates of the meteor point are 3.60° W, 39.37° N, height = 25 km.

The next procedure was to assume several possible azimuths of the fireball radiant and to check how compatible the resulting trajectory is with the visual observations and the Ciudad Real train image. In the following, we use the astronomical azimuths (South = 0, West = 90°, North = 180°, East = 270°). The Parla image and visual data show that the fireball flew nearly from the east to the west. We therefore tried trajectory azimuths 250, 270, and 290 degrees. The vertical plane containing the above-determined meteor point and the direction to the given azimuth was constructed for each azimuth. The intersection of that plane with the Parla plane then defines the fireball trajectory. The slope of the trajectory (elevation of the radiant) is determined automatically for any chosen azimuth by the Parla plane.

Unfortunately, eight of twelve eyewitness sites lie very close to (within 10 km of) the Parla plane. This means that even if we had very good data from those sites, the combination with the Parla train observation would not give the trajectory solution. Moreover, most of the visual data are of limited quality and lie quite far from all possible solutions. Only three sites lie more than 100 km from the Parla plane. The data from Alcantarilla seem to favor trajectories with lower azimuths, while the data from Soneja favor higher azimuths. Both these observations are compared to the possible fireball paths in Fig. 7. The data from the third site (Dúdar) were not good enough to judge.

Different trajectory solutions were also compared with the observed strewn field. Simulated meteorites were launched from the positions of train knots 1–9 (see the knot coordinates and heights in Table 3) in the direction of fireball flight (see Table 5 for radiant elevations; for azimuth 250°, the elevation was 39.9°) with a velocity of 4 km/s and decelerations corresponding to meteorite masses in the 1–100 g range. The dark flight was computed with the method of Ceplecha (1987) assuming spherical meteorite shapes and considering atmospheric winds shown in Fig. 6. The results are given in Fig. 8. Larger meteorites were generally predicted to lie further downrange (to the West) but because meteorites were launched from various heights, meteorite masses were partly mixed.

Since not all land was equally suitable for meteorite searches, the distribution of recovered meteorites is affected by selection effects. The trajectory with azimuth 290° produces the best match to the observed meteorite strewn field, although the trajectory azimuth 250° is not completely impossible considering the large meteorite scatter and the selection effects of the searches.

Finally, we can check the position of the train on the Ciudad Real images (Fig. 9). Ciudad Real lies only 3 km from the Parla plane, so the predicted train positions for different trajectory solutions follow almost the same path. The only difference is that a lower radiant azimuth gives a shorter train as seen from Ciudad Real. The knots seen from Parla should therefore appear closer together for smaller radiant azimuths than for larger azimuths. The expected positions of the knots for the moment of train formation and for the time 6 minutes later were computed, assuming that the knots move horizontally with the wind. Since the train was located to the northeast from Ciudad Real and the prevailing winds were from northwest, all knots are expected to move to the right. The amount of the movement is slightly different for different trajectory solutions since different solutions project the knots to different heights (see Table 3).

The measured train position from Parla does not match any of the solutions. The train clouds were observed significantly higher above the horizon. The possible explanation is that the train knots, which later developed into the clouds, moved not only horizontally with the wind but also vertically upwards. The upward movement is suggested also by the comparison of the positions of the clouds seen well

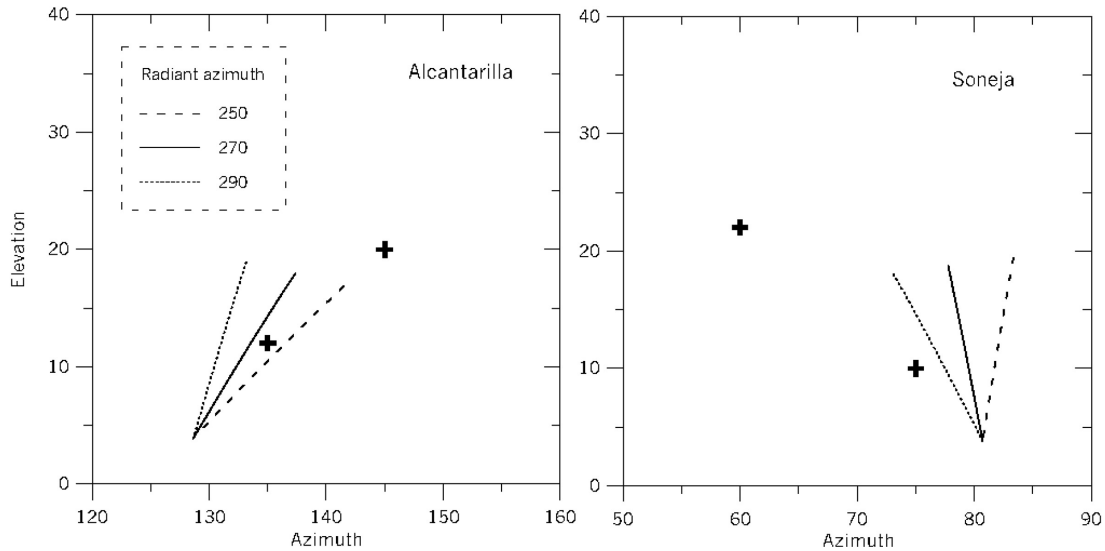


Fig. 7. Comparison of visual observations with three fireball trajectory solutions (for radiant azimuths 250, 270, and 290 degrees). The possible fireball paths at two observing sites are shown as dashed, solid, and dotted lines. The length of the lines corresponds to fireball heights from 80 km to 25 km. The fireball beginnings and ends reported by visual observers are given as crosses. The visual observations are evidently of low accuracy.

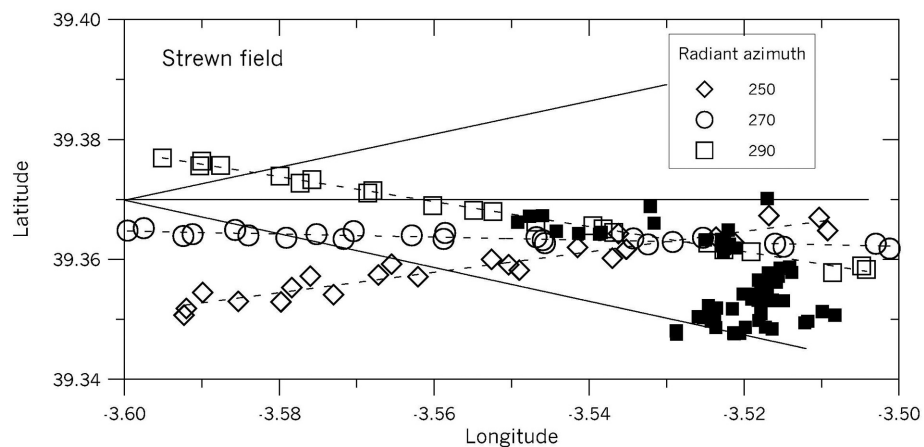


Fig. 8. The observed and simulated meteorite strewn field. The positions of recovered meteorites are given as black squares. The simulated landing points of meteorites of various masses launched at various heights are given as empty symbols. Different symbols represent different trajectory solutions (radiant azimuths). The scatter of the points reflects only the varying wind at various heights affecting fragments of different sizes. The real scatter will be larger because of impulses gained by the meteorites during atmospheric fragmentation and because of their irregular shapes. The solid lines represent ground projections of the trajectories.

on the two train images taken from Ciudad Real (knots D, E, F, G, H in Figs. 4a and 4b).

Unfortunately, it is difficult to decide which of the trajectory solutions is the best. The mutual identifications of the Parla knots with Ciudad Real clouds are not certain. It is likely that cloud F or G corresponds to knot 6. It is not clear if the cloud A corresponds to knot 0, whose existence is uncertain, or to knots 1 or 2. Knots 1 and 2 seem to correspond better with clouds D and E. The trajectory solutions with larger radiant azimuths seem to be closer to the Ciudad Real train observations, but it is difficult to say without further knowledge of how the train evolved. The train cloud coordinates as seen from Ciudad Real are given in Table 4.

DISCUSSION: PROBABLE TRAJECTORY AND HELIOCENTRIC ORBIT

None of our data strictly restrict the radiant azimuth, although most of them (except the visual observation from Alcantarilla) favor trajectories with larger azimuths. The uncertainty remains large so we can only say that the radiant azimuth lay in the range $260\text{--}290^\circ$. In other words, the azimuth was $275 \pm 15^\circ$. The values of other parameters of the trajectory corresponding to different azimuths are given in Table 5. All solutions pass through a point with longitude -3.600° , latitude 39.370° , height = 24.93 km (the meteorite point). Of course, the real uncertainty of this point, which is

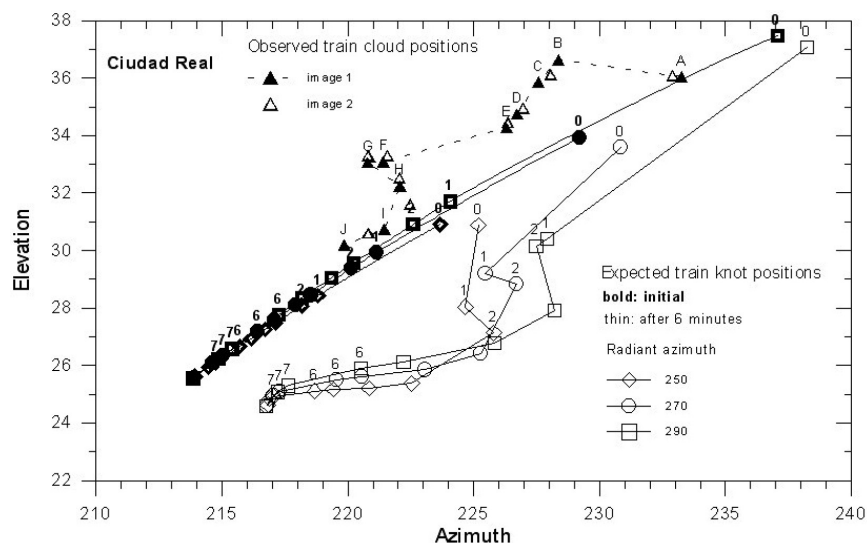


Fig. 9. The measured positions of the train clouds on the Ciudad Real images (triangles), the predicted positions of the train knots (as seen on the Parla image) at the moment of train formation (bold diamonds, circles, and squares- different symbols for different trajectory solutions) and after 6 minutes of wind drift (thin symbols).

Table 3. Azimuths and elevations of the train knots seen from Parla and their geographical coordinates for three trajectory solutions (latitudes and longitudes are expressed in degrees; heights in kilometers).

Knot no.	Azim.	Elev.	Assumed radiant az = 250			Assumed radiant az = 270			Assumed radiant az = 290		
			Long.	Lat.	Heig.	Long.	Lat.	Heig.	Long.	Lat.	Heig.
0	340.69	22.77	3.392	39.428	40.95	3.366	39.370	43.99	3.332	39.294	47.92
1	347.25	17.68	3.511	39.395	31.75	3.504	39.370	32.71	3.496	39.340	33.85
2	347.94	17.07	3.525	39.391	30.74	3.519	39.370	31.53	3.512	39.345	32.45
3	349.12	16.21	3.545	39.385	29.14	3.541	39.370	29.68	3.537	39.352	30.31
4	349.48	15.80	3.553	39.383	28.55	3.550	39.370	29.01	3.546	39.355	29.52
5	350.09	15.38	3.563	39.380	27.76	3.561	39.370	28.10	3.558	39.358	28.49
6	350.51	15.00	3.571	39.378	27.13	3.570	39.370	27.39	3.568	39.361	27.69
7	351.50	14.37	3.588	39.373	25.87	3.587	39.370	25.97	3.586	39.366	26.09
8	351.68	14.06	3.593	39.372	25.50	3.592	39.370	25.56	3.592	39.368	25.63
9	352.17	13.68	3.601	39.370	24.82	3.601	39.370	24.81	3.602	39.370	24.80

Table 4. Measured positions of train clouds on two images from Ciudad Real.

Cloud	Image 1		Image 2	
	Azim. (°)	Elev. (°)	Azim. (°)	Elev. (°)
A	233.26	36.04	232.90	36.08
B	228.36	36.65		
C	227.56	35.86	228.06	36.11
D	226.72	34.75	226.97	34.95
E	226.29	34.27	226.35	34.46
F	221.41	33.09	221.58	33.30
G	220.78	33.07	220.80	33.32
H	222.06	32.25	222.04	32.54
I	221.47	30.75	222.47	31.62
J	219.86	30.18	220.81	30.61

based on the positions of recovered meteorites, is a few kilometers.

The heliocentric orbit of the meteoroid would be of great interest. The accurate reconstruction of the original orbit in

the solar system of a meteorite has been obtained only on nine occasions. It is logical that such a small sample is strongly biased towards the most common meteorite classes. In fact, seven of those meteorites are ordinary chondrites: Příbram (Ceplecha 1961), Lost City (McCrosky et al. 1971), Innisfree (Halliday et al. 1978), Peekskill (Brown et al. 1994), Morávka (Borovička et al. 2003), Park Forest (Brown et al. 2004), and Villalbeto de la Peña (Trigo-Rodríguez et al. 2006). Two more recent falls have provided information about other meteorite types: the carbonaceous chondrite Tagish Lake (Brown et al. 2002), and the Neuschwanstein enstatite chondrite (Spurný et al. 2003). The heliocentric orbit of the Puerto Lápice fireball cannot be computed because there is no information on fireball velocity. Despite this, we can map the possible extent of orbital elements by using the possible fireball radiants from Table 5 and various velocities. The results shown in Table 6 indicate that the fireball was on an Apollo-type orbit with semi-major axis larger than 1 AU (i.e., not

Table 5. The range of possible radiant coordinates and trajectory beginnings (for the fixed height 80 km).

Apparent radiant				Beginning point (h = 80 km)	
Azimuth	Elevation	Right ascension	Declination	Longitude	Latitude
260.0	42.0	192.9	31.6	-2.912	39.462
275.0	43.4	185.4	22.8	-2.939	39.323
290.0	42.8	178.8	13.7	-2.965	39.188

Table 6. Computed orbital elements (J2000.0) for the probable range of radiant azimuths and several possible pre-atmospheric velocities of the fireball.

Radiant azimuth (°)	Velocity (km/s)	a (AU)	e	q (AU)	Q (AU)	ω (°)	Ω (°)	i (°)
260	11.5	1.01	0.03	0.989	1.04	262.0	49.641	1.2
260	12	1.10	0.11	0.975	1.23	228.1	49.615	3.6
260	15	1.80	0.46	0.970	2.64	209.0	49.607	8.8
260	18	4.0	0.76	0.967	7.1	205.6	49.606	11.7
275	12	1.14	0.14	0.980	1.3	219.7	49.625	2.1
275	15	2.09	0.54	0.972	3.2	207.0	49.610	5.6
275	18	6.7	0.86	0.968	12.5	204.6	49.608	7.6
290	12	1.17	0.16	0.983	1.37	215.5	49.713	0.4
290	15	2.32	0.58	0.974	3.67	205.4	49.622	2.3
290	18	12.0	0.92	0.970	23.1	203.5	49.616	3.4
Summary		>1	Any	$0.98 \pm .02$	>1	203–230	49.6–49.7	<12

on Aten-type orbit with $a < 1$). The actual value of the semi-major axis strongly depends on assumed velocity and could not be determined. The perihelion distance was only slightly lower than 1 AU, between 0.965 and 1 AU. The inclination was lower than 12° . The orbits in Table 6 with aphelion smaller than 1.1 AU or larger than 5 AU can be considered improbable.

Asteroid 4 Vesta was postulated to be the parent body of HED meteorites due to two unique spectral features in its reflectance spectrum (McCord et al. 1970; Larson and Fink 1975). Consolmagno and Drake (1977) proposed that Vesta is the most likely source of HED meteorites due to its survival until the present time. A systematic identification of a number of small asteroids with Vesta-like spectra that were called Vestoids was made by Binzel and Xu (1993) and later revisited by Burbine et al. (2001). Puerto Lápice orbital data is giving some insight on this exciting topic. Some of the orbital solutions (especially those for a geocentric velocity of 15 km/s) are showing that the progenitor meteoroid would be coming from the lower limit of semi-major axis of the Vesta family that is located at 2.47 AU, near the 3:1 resonance (Burbine et al. 2001). Of course, the absence of velocity data makes it impossible to discard its provenance from the ν_6 resonance that is in the upper limit of the family. It is important to remark that the 3:1 main Jovian resonance has been previously identified as one of the main sources for delivering meteorites to the Earth. In fact, among the meteorite orbits with semi-major axes of ~ 2.5 and eccentricities of ~ 0.6 that would be suggesting a delivery by the 3/1 resonance, we find Příbram, Neuschwanstein, Park Forest and Villalbeto de la Peña

(Ceplecha et al. 1961; Spurný et al. 2003; Brown et al. 2004; Trigo-Rodríguez et al. 2006).

All previously determined orbits of meteorites point to the main resonances in the asteroidal belt as the source of meteorites, although near-Earth objects (NEOs) would also contribute (Trigo-Rodríguez et al. 2007). It is clear that the only way to increase our data on the dynamic mechanisms that are sending meteorites toward the Earth is by increasing our efforts to collect as much information as possible of meteorite falls, and particularly on those meteorite classes that are unusual and rarely observed. The Puerto Lápice eucrite is a clear example of these rare falls, having Pasamonte as the only precedent (Nininger 1936). As in all the previous HED falls the compilation of trajectory information was marginal or nonexistent; the data obtained here for the Puerto Lápice daylight fireball are especially relevant.

CONCLUSIONS

The Puerto Lápice event is the first eucrite-dropping fireball whose trajectory has been reconstructed so far with some reliability. On the basis of the trajectory data obtained we estimated a range of orbital solutions. Although no velocity information was obtained from the casual reports of the event, the data compiled allowed the determination of a range of orbital elements. These data indicate that the fireball was on a Apollo-type orbit with semi-major axis larger than 1 AU. The original meteoroid could have been delivered from the main belt by a resonance, but this hypothesis clearly needs further study on the basis of accurate orbital data of future HED falls. In such speculative context, the 3:1 and ν_6

resonances would link the Puerto Lápice meteoroid to the Vesta family and this would provide a similar delivery source to that of previous cases of meteorites with reasonably well determined orbits.

Acknowledgments—We thank the referee, Prof. Jürgen Oberst, for very useful comments on an earlier draft of this paper. We acknowledge funding from MEC AYA2007-30476-E (Spain). We thank Bartolomé Orfila and Juan Guerra Gómez (Instituto Nacional de Meteorología) for providing us with an accurate sounding model of the wind pattern for the exact coordinates and date of the fall. The Seismologic Network of the Instituto Geográfico Nacional kindly provided us with the seismic records, although the sound of this bolide event was not positively identified. We also thank the effort made by SPMN collaborators participating in theodolite measurements and meteorite recovery: José V. Casado, Antonio Garrido, Francisco Ocaña, Berenice Pila, Antonio Rodríguez, Antonio del Solar, Alejandro Sánchez, and Carlos E. Tapia. Members of the Agrupación Astronómica de Madrid (AAM) and Asociación de Astrónomos Aficionados de la Universidad Complutense de Madrid (ASAAF-UCM) participated actively in the meteorite recovery. We thank Wayne Edwards (University of Western Ontario) for checking the seismic records and Alan Rubin (UCLA) for improving the language in the manuscript. Miguel A. Bajo, Manuel Trigo y Ramón Zaragoza kindly provided the pictures of the fireball's train, and facilitated the required details for allowing nocturnal calibrations. We would also like to express our gratitude to all eyewitnesses who reported their data to SPMN. Among them, we are grateful to those who showed SPMN researchers their observing locations for performing nocturnal calibrations, theodolite measurements or for obtaining additional data on the fireball. Our special thanks to J. Albarreal, P. Arguisuelas, Prof. J. Alba-Tercedor, M. A. Bajo, I. Barbero, A. Basanta, M. Castillo, J. Climent, J. Cuesta, J. Cuevas, M. Durán, F. Gómez, A. Gonzalo, M. Gete, M. Impastato, M. A. Martín, D. A. Farto, F. Gálvez, L. Gálvez, A. García, A. Hernández, C. Madruga, B. Mills, F. Molina, J. Núñez, M. Olcina, J. Ortiz, A. Pérez, M. A. Pérez, C. Plaza, S. Quicios, R. Ramos, C. Rodríguez, J. M. Salinas, A. Sánchez, M. T. Sánchez, A. M. Segovia, M. Serrano, J. Taltavull, M. Trigo, A. Valdepeñas, G. Vázquez, J. S. Wolf, T. Venemay, and R. Zaragoza. Other meteorite location information was kindly provided by meteorite dealers: Mike Farmer, Robert Haag, Siegfried Haberer, Thomas Grau, Moritz Karl, Robert Ward, and an anonymous.

Editorial Handling—Dr. Walter Huebner

REFERENCES

- Binzel R. P. and Xu S. 1993. Chips off of asteroid 4 Vesta: Evidence for the parent body of basaltic achondrite meteorites. *Science* 260:186–191.
- Borovička J., Spurný P., Kalenda P., and Tagliaferri E. 2003. The Morávka meteorite fall: I. Description of the events and determination of the fireball trajectory and orbit from video records. *Meteoritics & Planetary Science* 38:975–987.
- Britt D. T. and Consolmagno G. J. 2003. Stony meteorite porosities and densities: A review of the data through 2001. *Meteoritics & Planetary Science* 38:1161–1180.
- Brown P., Ceplecha Z., Hawkes R. L., Wetherill G., Beech M., and Mossman K. 1994. The orbit and atmospheric trajectory of the Peekskill meteorite from video records. *Nature* 367:624–626.
- Brown P. G., ReVelle D. O., Tagliaferri E., and Hildebrand A. R. 2002. An entry model for the Tagish Lake fireball using seismic, satellite, and infrasound records. *Meteoritics & Planetary Science* 37:661–675.
- Brown P. G., Pack D., Edwards W. N., ReVelle D. O., Yoo B. B., Spalding R. E., and Tagliaferri E. 2004. The orbit, atmospheric dynamics, and initial mass of the Park Forest meteorite. *Meteoritics & Planetary Science* 39:1781–1796.
- Burbine T. H., Buchanan P. C., Binzel R. P., Bus S. J., Hiroi T., Hinrichs J. L., Meibom A., and McCoy T. J. 2001. *Meteoritics & Planetary Science* 26:761–781.
- Ceplecha Z. 1961. Multiple fall of Příbram meteorites photographed. *Bulletin of the Astronomical Institute of Czechoslovakia* 12:21–47.
- Ceplecha Z. 1987. Geometric, dynamic, orbital and photometric data on meteoroids from photographic fireball networks. *Bulletin of the Astronomical Institute of Czechoslovakia* 38:222–234.
- Connolly H. C. Jr., Smith C., Benedix G., Folco L., Righter K., Zipfel J., Yamaguchi A., and Chennaoui Aoudjehane H. 2008. The Meteoritical Bulletin, No. 93. *Meteoritics & Planetary Science* 43:571–632.
- Consolmagno G. J. and Drake M. J. 1977. Composition and evolution of the eucrite parent body: Evidence from rare earth elements. *Geochimica et Cosmochimica Acta* 41:1271–1282.
- Consolmagno G. J., Macke R. J., Rochette P., Britt D. T., and Gattacceca J. 2006. Density, magnetic susceptibility, and the characterization of ordinary chondrite falls and showers. *Meteoritics & Planetary Science* 41:331–342.
- Grossman J. N. and Score R. 1996. The Meteoritical Bulletin, No. 79. *Meteoritics & Planetary Science* 31:A161–A180.
- Halliday I., Blackwell A. T., and Griffin A. A. 1978. The Innisfree meteorite and the Canadian camera network. *Journal of the Royal Astronomical Society of Canada* 72:15–39.
- Larson H. P. and Fink U. 1975. Infrared spectral observations of asteroid 4 Vesta. *Icarus* 26:420–427.
- Llorca J., Trigo-Rodríguez J. M., Ortiz J. L., Docobo J. A., García-Guinea J., Castro-Tirado A. J., Rubin A. E., Eugster O., Edwards W., Laubenstein M., and Casanova I. 2005. The Villabeto de la Peña meteorite fall: I. Fireball energy, meteorite recovery, strewn field and petrography. *Meteoritics & Planetary Science* 40:795–804.
- Llorca J., Casanova I., Trigo-Rodríguez J. M., Madiedo J. M., Roszjar J., Bischoff A., Ott U., Franchi I. A., Greenwood R. C., and Laubenstein M. 2008. The Puerto Lápice eucrite. *Meteoritics & Planetary Science* 44. This issue.
- Madiedo J. M., Trigo-Rodríguez J. M., Llorca J., Borovička J., Zamorano J., Izquierdo J., and Ocaña F. 2008. The Puerto Lápice eucrite fall phenomenon (abstract #1815). 39th Lunar and Planetary Science Conference. CD-ROM.
- McCord T. B., Adams J. B., and Jhonson T. V. 1970. Asteroid Vesta: Spectral reflectivity and compositional implications. *Science* 168:1445–1447.
- McCrosky R. E., Posen A., Schwartz G., and Shao C.-Y. 1971. Lost City meteorite: Its recovery and a comparison with other fireballs. *Journal of Geophysical Research* 76:4090–4108.
- Nininger H. H. 1936. The Pasamonte, New Mexico, meteorite. *Popular Astronomy* 47:331–337.

- Spurný P., Oberst J., and Heinlein D. 2003. Photographic observations of Neuschwanstein, a second meteorite from the orbit of the Příbram chondrite. *Nature* 423:151–153.
- Trigo-Rodríguez J. M., Borovička J., Spurný P., Ortiz J. L., Docobo J. A., Castro-Tirado A. J., and Llorca J. 2006. “The Villalbeto de la Peña meteorite fall: II. Determination of the atmospheric trajectory and orbit. *Meteoritics & Planetary Science* 41:505–517.
- Trigo-Rodríguez J. M., Lyttinen E., Jones D. C., Madiedo J. M., Castro-Tirado A., Williams I., Llorca J., Viték S., Jelínek M., Troughton B., and Gálvez F. 2007. Asteroid 2002NY40 as source of meteorite-dropping bolides. *Monthly Notices of the Royal Astronomical Society* 382:1933–1939.
- Trigo-Rodríguez J. M., Rietmeijer F. J. M., Llorca J., and Janches D. 2008. Preface. Meteoroids 2007 Conference, *Earth Moon and Planets*, doi:10.1007/s11038-008-9228-0.
-